Supplementary Information for

Highly Efficient Hamburger-like Nanostructure of Triadic $Ag/Co_3O_4/BiVO_4$ Photoanode for Enhanced Photoelectrochemical Water Oxidation

Xintong Gao[ab], Zhiqun Bai[a], Shuai Zhang[c], Jingchao Liu*[a] and Zenghe Li *[b]

[a] *State Key Laboratory of Chemical Resource Engineering, Beijing University of Chemical Technology, Beijing 100029, China.*

[b] *Key Laboratory of Environmentally Harmful Chemical Analysis, College of Chemistry, Beijing University of Chemical Technology, Beijing, 100029, China.*

[c] *Key Laboratory of Photochemical Conversion and Optoelectronic Materials, Technical Institute of Physics and Chemistry, Chinese Academy of Sciences, Beijing, 100190, China*

**Corresponding author. E-mail: Jingchaoliu1992@163.com；lizh@mail.buct.edu.cn.*

Experimental sections

Chemicals

$Bi(NO_3)_3·5H_2O$, $Co(NO_3)_2·6H_2O$, $AgNO_3$, NaOH, NH_4F, $Na_3C_6H_5O_7·2H_2O$ (sodium citrate), Urea, Ethylene glycol (EG), Dimethyl sulfoxide (DMSO) were purchased from Sinopharm Chemical Reagent (Beijing Co., Ltd.). Vanadium (Ⅲ) acetylacetonate ($VO(acac)_2$) was purchased from Shanghai Aladdin Bio-Chem Technology Co., Ltd. All reagents were of analytical grade and were used without further purification. Deionized water was used throughout the experiments. FTO substrates (F: SnO_2, 1cm*3cm, 14 $m\Omega·cm^{-2}$) were received from Wuhan GeAo teaching instruments co., Ltd.

Characterizations

Crystallographic information for the samples was collected using X-ray diffraction (XRD, Rigaku D/MAX-2500 diffractometer, copper Kα radiation with λ = 0.154 nm). The X-ray photoelectron spectra (XPS) were recorded on a VGESCALAB-MK electron spectrometer with Al Kα as the excitation source. SEM images were obtained by field emission scanning electron microscopy (FESEM, Zeiss Supra 55, on 20.0 kV). High resolution transmission electron microscopy (HRTEM) images were noted on JEOL JEM-2010 microscopy with an accelerating voltage of 200 kV. Solid-state UV-Vis absorption spectra were measured at room temperature by using a spectrometer equipped with an integrating sphere attachment (Shimadzu UV-3000) by using $BaSO_4$ as a background sample. The signal from the FTO conductive glass was subtracted.

Photoelectrochemical measurements

For PEC tests, the measurements were conducted on a three-electrode configuration in a quartz cell. The prepared heterojunction working electrode with $2cm^2$ exposure area was placed into a cell with a Pt counter electrode and Ag/AgCl reference electrode, respectively. The cell was filled with 0.1 M phosphate buffer solution (shorthand for PBS, pH = 7), and the light source employed in PEC tests was a 500W Xenon lamp with an AM 1.5 G filter. The linear sweep voltammograms were operated at 20 mV s^{-1} in a potential range from -0.4 to 1.2 V vs Ag/AgCl both in dark and under illumination. All potentials mentioned were converted into the potential versus RHE (in volt) according to Eq. (1):

$$E_{RHE} = E_{Ag/AgCl} + E_{Ag/AgCl\ vs\ NHE} + 0.059\text{pH} \qquad (1)$$

The $E_{Ag/AgCl\ vs\ NHE}$ (versus normal hydrogen electrode) in Eq. (1) is 0.197 V at 20 °C.

Electrochemical impedance spectroscopy (EIS) was performed on the electrochemical workstation mentioned above at an open circuit voltage of 1.23 V vs RHE under illumination with 0.1V amplitude of perturbation and a frequency between 100 kHz and 0.1 Hz. The measured impedance data were fit to an appropriate equivalent circuit using the Zview software package (version

3.2c) to derive the resistance values. Mott−Schottky plots were measured at room temperature in the dark.

The incident photon to electron conversion efficiency (IPCE) of the samples was measured under monochromatic light illumination at 1.23 V *vs.* RHE. Monochromatic light was generated using the Oriel Cornerstone 130 monochromator, and the output power was measured using a photodiode detector. IPCE was calculated using Eq. (2):

$$IPCE = (1240J) / (\lambda \cdot P_{light}) \quad (2)$$

Where J is the measured photocurrent density (mA cm^{-2}), λ is the wavelength of the incident light (nm) and P is the power density of monochromatic light at each wavelength (mW cm^{-2}).

The photoconversion efficiency (η) was calculated using Eq. (3):

$$\eta = J\,(1.23 - E_{RHE})/P_{light} \quad (3)$$

Intensity-modulated photocurrent spectroscopy (IMPS) measurements were conducted with a potentiostat (IM6ex, Zahner Co.) controlled by a Zahner IMPS electrochemical workstation. Intensity-modulated light was provided by a lightemitting diode (LED) that allowed superimposition of sinusoidal modulation (~10%) on a dc illumination level. The wavelength of light was 430 nm with an average intensity of 2 mW cm^{-2}, and the modulation amplitude of lamp voltage was 10 mV. The photocurrent as a function of frequency (from 0.1 Hz to 5k Hz) after the light was turned on was recorded. Electron transfer time τ_d was calculated according to Eq. (4):

$$\tau_d = (2\pi \cdot f_{min})^{-1} \quad (4)$$

Where f_{min} is the frequency value of the lowest point in the semicircle of the test.

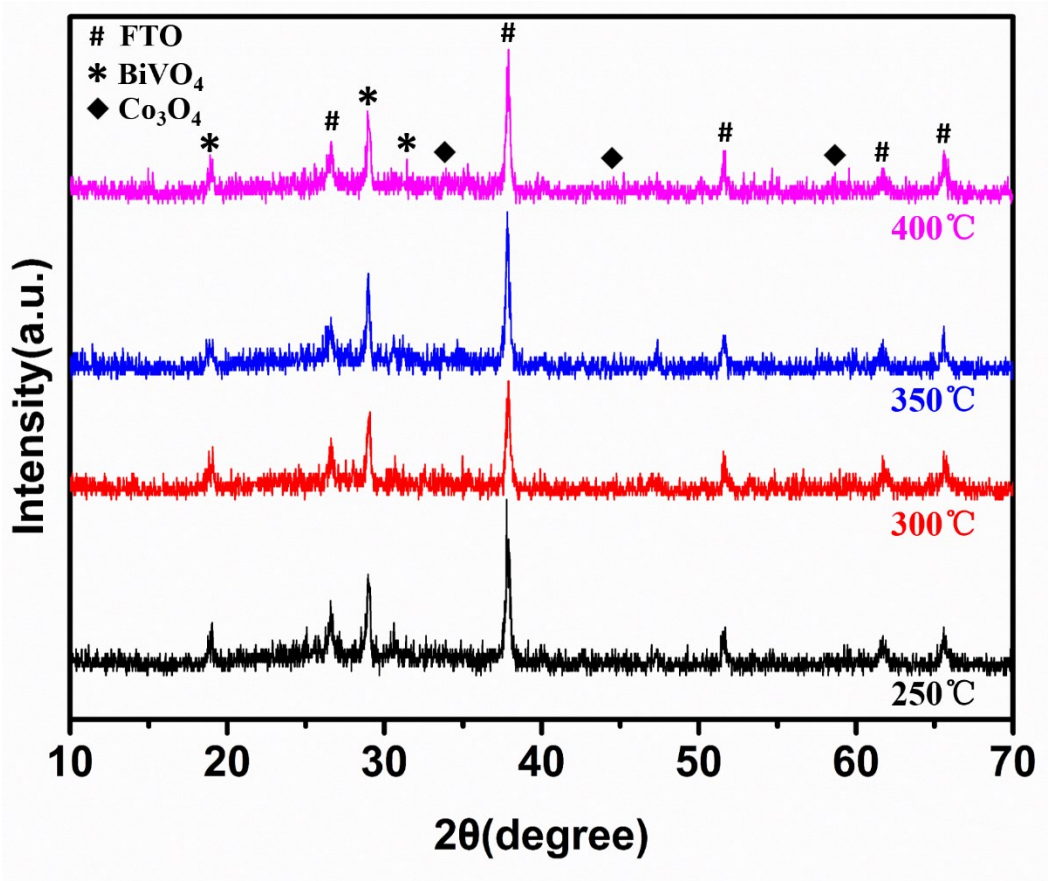

Fig. S1 XRD patterns of Co_3O_4/$BiVO_4$/FTO with different calcination temperatures for Co_3O_4 layer.

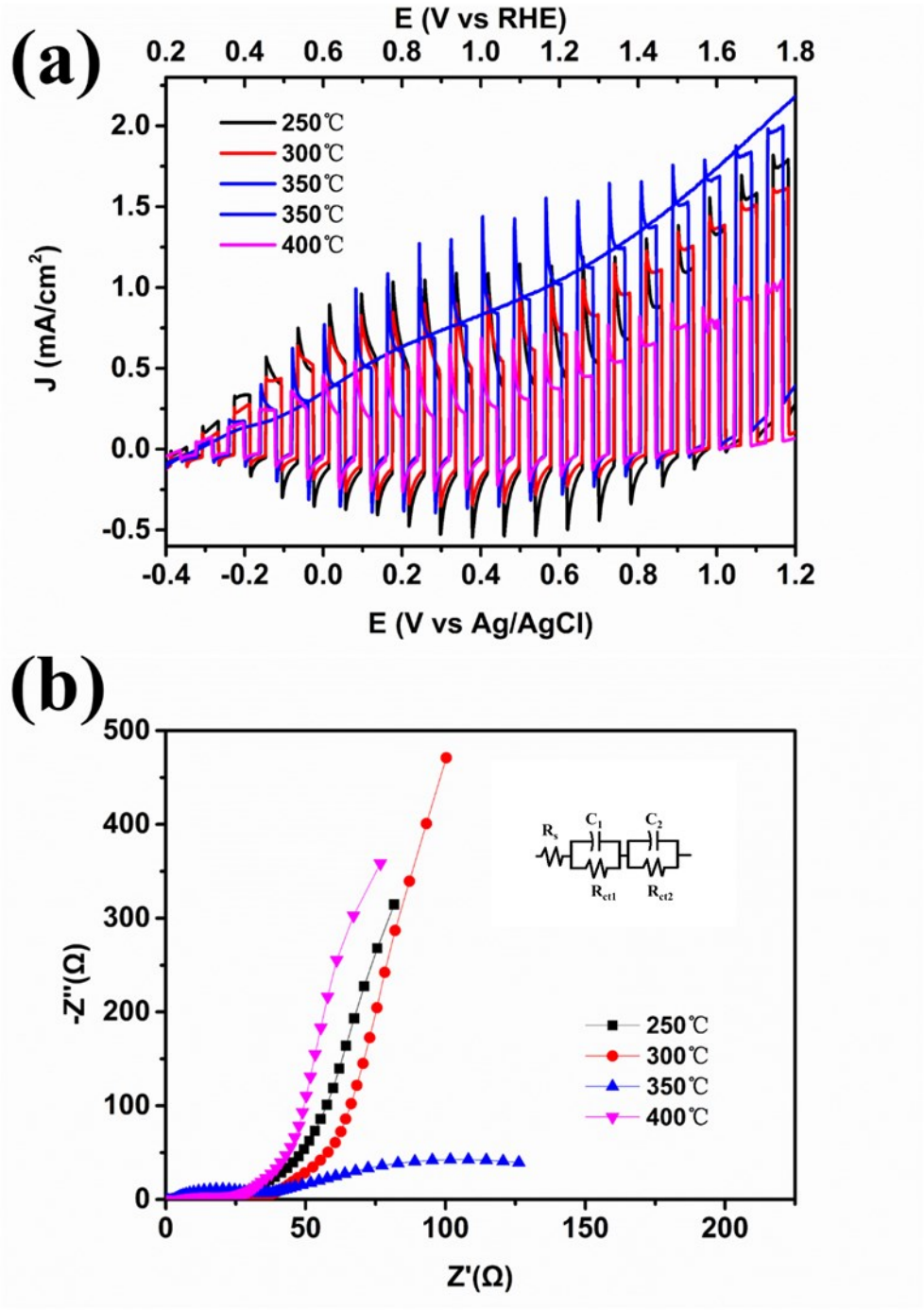

Fig. S2 (a) Current−potential curves under chopped AM1.5G illumination; (b) Nyquist plots of the $Co_3O_4/BiVO_4$ photoanodes with different calcination temperatures for Co_3O_4 layer.

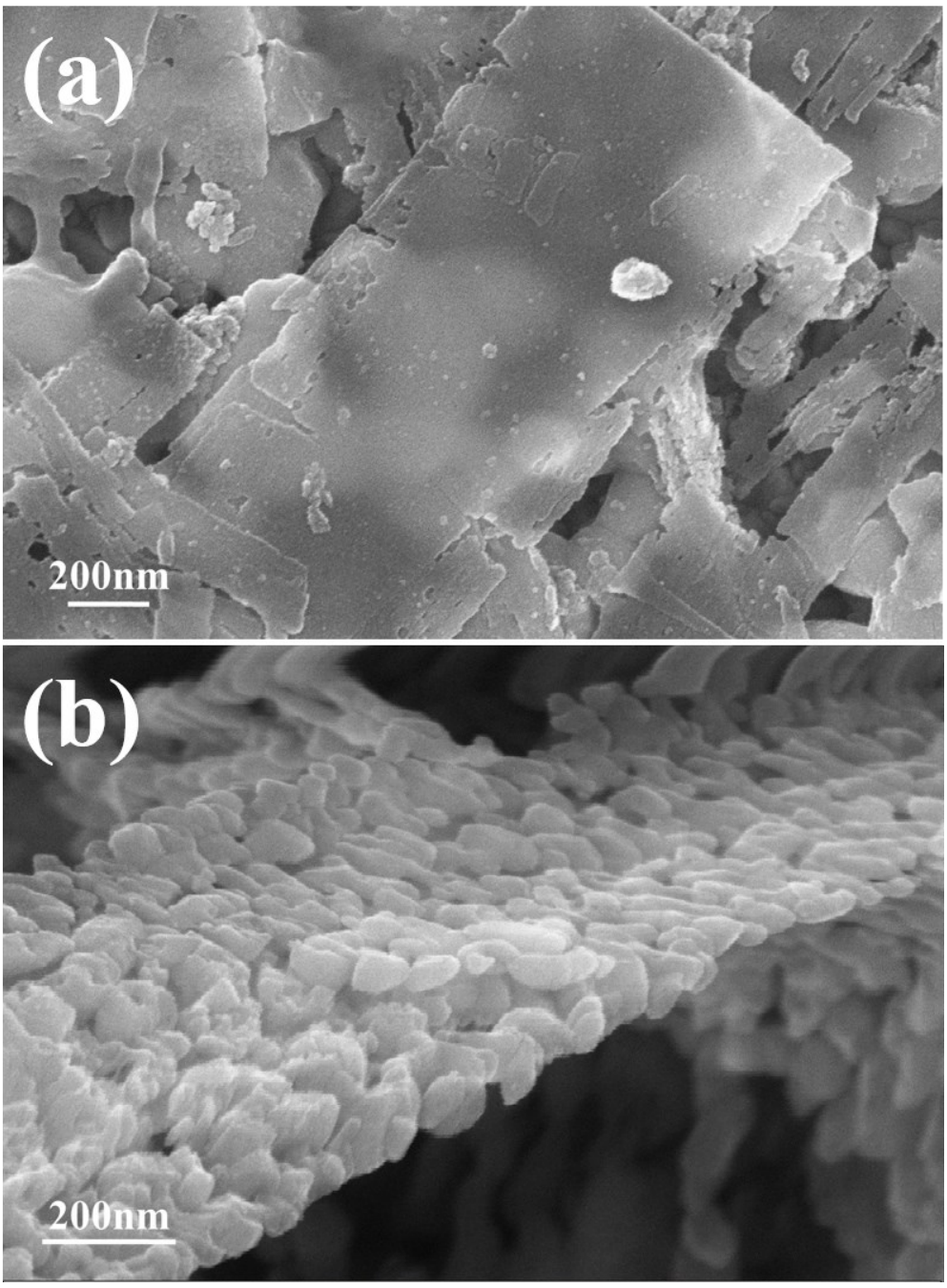

Fig. S3 SEM images of $Co_3O_4/BiVO_4$ photoanode with (a) 350 °C and (b) 400 °C calcination for Co_3O_4 layer.

As shown in Fig. S2a, the current-potential curves of the photoanodes (prepared at 250^{o}C, 300^{o}C, 350^{o}C and 400^{o}C, respectively) were measured under chopper illumination. As the temperature increased, the photocurrent response of the $Co_3O_4/BiVO_4$ photoanode increased. The strongest photocurrent response was reached in the $Co_3O_4/BiVO_4$ photoanode prepared at 350 °C. The higher temperature (400 °C) was used to synthesize the $Co_3O_4/BiVO_4$ photoanode that exhibited significantly

suppressed photocurrent response. The EIS (Fig. S2b) test showed that as the temperature increased, the semidiameter of the $Co_3O_4/BiVO_4$ photoanode decreased. At 350 °C, the $Co_3O_4/BiVO_4$ photoanode afforded the smallest half diameter and the best PEC. However, at higher temperatures (400 °C), the semidiameter of the $Co_3O_4/BiVO_4$ photoanode increased, and its PEC activity became worse. It is assumed that the Co_3O_4 formed at low temperature may possess poor crystallinity and inefficient charge separation/transfer performance, while a higher temperature may cause the Co_3O_4 layer broken (Fig. S3). Based on the above experimental results and discussion, 350 °C was determined to the optimal calcining temperature for the formation of the $Co_3O_4/BiVO_4$ photoanode.

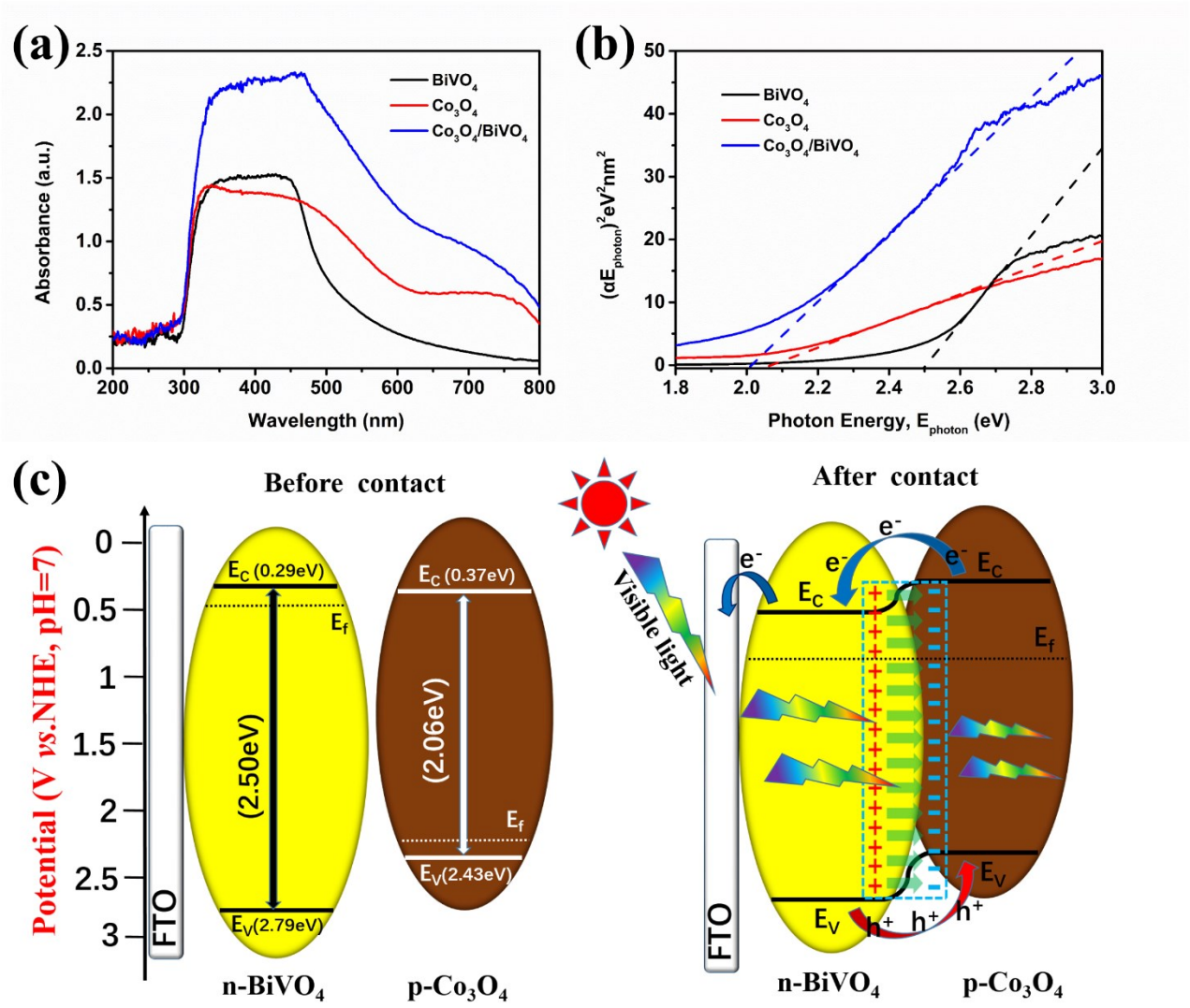

Fig. S4 (a) Diffuse reflectance spectra of $BiVO_4$, Co_3O_4 and $Co_3O_4/BiVO_4$.(b) Bandgap energy of $BiVO_4$, Co_3O_4 and the $Co_3O_4/BiVO_4$ heterojunction. (c) Schematic energy diagram and charge transfer between p-type Co_3O_4 and n-type $BiVO_4$.

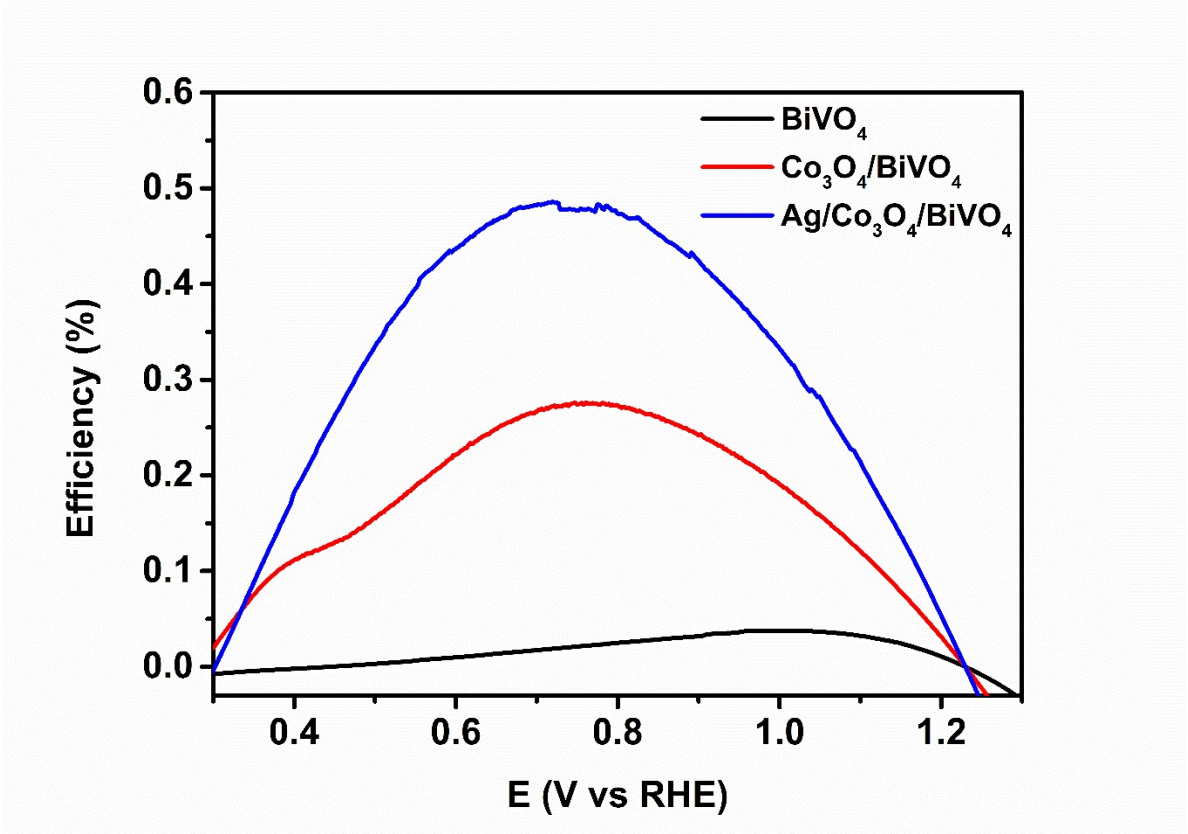

Fig. S5 Photoconversion efficiency as a function of applied voltage.

Table S1 Nyquist plot fitted results in Ω of 1 mM, 2mM, 3mM, 4mM $Co_3O_4/BiVO_4$ photoanodes.

Sample	R_s	R_{ct1}	R_{ct2}
1 mM $Co_3O_4/BiVO_4$	43.00	46.75	367.90
2 mM $Co_3O_4/BiVO_4$	37.22	34.64	363.35
3 mM $Co_3O_4/BiVO_4$	48.18	70.96	181.00
4 mM $Co_3O_4/BiVO_4$	42.02	29.00	1192

R_s is defined as the series resistance, R_{ct1} in low impedance (high frequency) represents charge transfer resistance across the interface between the semiconductors, R_{ct2} in high impedance (low frequency) is the charge transfer resistance across the electrode/electrolyte interface.[1-3]

Table S2 Nyquist plot fitted results in Ω of $BiVO_4$, $Co_3O_4/BiVO_4$, $Ag/Co_3O_4/BiVO_4$ photoanodes.

Sample	R_s	R_{ct1}	R_{ct2}
$BiVO_4$	54.30	136.80	502.90
$Co_3O_4/BiVO_4$	48.18	70.96	181.00
$Ag/Co_3O_4/BiVO_4$	53.84	—	180.60

R_s is defined as the series resistance, R_{ct1} in low impedance (high frequency) represents charge transfer resistance across the interface between the semiconductors, R_{ct2} in high impedance (low frequency) is the charge transfer resistance across the electrode/electrolyte interface.[1-3]

References

1 G. Liu, Y. Zhao, K. Wang, D. He, R. Yao and J. Li, *ACS Sustain. Chem. Eng*, 2018, **6**, 2353-2361.

2 S. S. M. Bhat, S. A. Lee, T. H. Lee, C. Kim, J. Park, T.-W. Lee, S. Y. Kim and H. W. Jang, *ACS Appl. Energy Mater.*, 2020, **3**, 5646-5656.

3 X. Zhang, X. Wang, X. Yi, J. Ye and D. Wang, *ACS Sustain. Chem. Eng*, 2019, **7**, 5420-5429.